

AQP and the Control of Fluid Transport in a Salivary Gland

M. Murakami¹, K. Murdiastuti^{2,3}, K. Hosoi², A.E. Hill⁴

¹Center for Integrative Bioscience, NIPS, National Institute for Natural Sciences, Myoudaiji, Okazaki 444-8787, Japan

²Department of Physiology and Oral Physiology, Tokushima University School of Dentistry, Tokushima-Shi, Tokushima 770-8504, Japan

³Department of Periodontology, Gadjah Mada University Faculty of Dentistry, Yogyakarta 55281, Indonesia

⁴Physiological Laboratory, University of Cambridge, Downing St., Cambridge CB2 3EG, UK

Received: 16 January 2006

Abstract. Experiments were performed with the perfused rat submandibular gland *in vitro* to investigate the nature of the coupling between transported salt and water by varying the osmolarity of the source bath and observing the changes in secretory volume flow. Glands were submitted to hypertonic step changes by changing the saline perfusate to one containing different levels of sucrose. The flow rate responded by falling to a lower value, establishing a new steady-state flow. The rate changes did not correspond to those expected from a system in which fluid production is due to simple osmotic equilibration, but were much larger. The changes were fitted to a model in which fluid production is largely paracellular, the rate of which is controlled by an osmosensor system in the basal membrane. The same experiments were done with glands from rats that had been bred to have very low levels of AQP5 (the principal aquaporin of the salivary acinar cell) in which little AQP5 is expressed at the basal membrane. In these rats, salivary secretion rates after hypertonic challenges were small and best modelled by simple osmotic equilibration. In rats which had intermediate AQP5 levels the changes in flow rate were similar to those of normal rats although their AQP5 levels were reduced.

Finally, perfused normal glands were subject to retrograde ductal injection of salines containing different levels of Hg^{2+} ions (0, 10 and 100 μM) which would act as inhibitors of AQP5 at the apical acinar membrane. The overall flow rates were progressively diminished with rising Hg^{2+} concentration, but after hypertonic challenge the changes in flow rates were unchanged and similar to those of normal rats.

All these results are difficult to explain by a cellular osmotic model but can be explained by a model

in which paracellular flow is controlled by an osmosensor (presumably AQP5) present on the basal membrane.

Key words: Salivary gland — Aquaporins — Osmosensors — Tight junctions — Water permeability — Paracellular system

Introduction

In previous experiments with the perfused *in vitro* rat submandibular gland (SMG) the paracellular transport of a series of molecular probes, ³H-labelled dextrans, was followed after stimulation of fluid transport [18]. The results showed that the fraction of the transepithelial volume flow that accompanies the net flux of probes across the tight junction and interspace system is close to 1.0 and therefore virtually all the water flow across the acinar epithelial cells is paracellular in nature. This result is incompatible with the theory of fluid production by osmotic equilibration, but similar results have been obtained for every epithelium in which the flux of paracellular probes has been followed. In rabbit gallbladder [28] and rabbit SMG [1] the paracellular water fraction is high and in systems where the fraction has been quantitatively determined it ranges from 0.98–1.0 in *Necturus* gallbladder [7, 25], 0.98–1.1 in *Necturus* intestine [11] and 1.0 in *Rhodnius* Malpighian tubule [6]. A model incorporating all the features of this flow was put forward but how it is controlled and co-ordinated with the cellular pumping of ions was not suggested at that time [10]. The evidence for paracellular fluid flow has been reviewed in detail recently [26].

With the rise of interest in aquaporins it has been natural to assume that their presence in epithelial membranes is to provide a set of channels for water

flow during fluid secretion. This would seem to lend weight to the theory of fluid production by osmotic equilibration, which was first advanced to explain the fact that the fluid is isotonic to the source bath [2, 4]. Detailed studies on epithelial fluid transport with knockout mice have been made recently [33–35] but it is only in a small minority of cases that the osmotic theory (as opposed to the contribution of aquaporins to membrane water permeability) can be supported. These cases are proximal tubule [24, 31] airway glands [27] and, most pertinently, salivary glands [15] although in all these cases the salt is also reduced by the knockout, for which there is no explanation. In fact, the reduction in salt extrusion would be enough to explain most of the reduction in fluid flow, within the osmotic theory, without involving aquaporins. These important results have been reviewed in detail along with other tissue knockouts and it has been concluded that they do not support cellular osmosis but reflect a more complex state of affairs [13].

It has been suggested that aquaporins may have a role as osmosensors and a possible mechanism has been described [13]. This was suggested by the interesting fact that they are always tetrameric, and might function as a quaternary assembly whose configuration is altered by a trans-membrane osmotic gradient. If this is correct, then in epithelia they are prime candidates for controlling the activity of the paracellular flow system. They would act as a feedback system, sensing the osmotic gradient and adjusting the paracellular flow to match the rate of salt pumping across the cell to give a quasi-isotonic fluid secretion. There are two problems faced by the osmotic theory of fluid secretion that apply to all epithelia with greater or lesser force. The first is that of the epithelial geometry; is the ‘coupling space’ adjacent to the membrane of sufficient size and shape to allow the transported salt to osmotically equilibrate before leaving the system? The second involves the magnitude of the osmotic permeability P_{os} . Given the geometry within which osmosis has to operate, is P_{os} high enough to achieve quasi-isotonicity? The two are connected and a current assumption is that aquaporins provide such a high value of P_{os} that they override the geometrical problem although there is no evidence that this is correct. The problems are very acute for the apical membrane of the salivary gland where the osmotic equilibration has to occur as fluid enters the lumen, but simple calculations show that there is little possibility of the secretion becoming isotonic before leaving the acinus unless the P_{os} of the apical membranes, whose area is relatively small, is enormous.

In this Issue a feedback model connecting salt pumping by the cell with paracellular fluid flow has been proposed in some detail [12]. An aquaporin, acting as an osmosensor, detects the difference in osmolarity between bath and cell and signals to a

junctional fluid transport system (the JFT system, a term used frequently throughout this paper) to set the rate of paracellular fluid transfer. This transfer is hypotonic because the JFT is more permeable to water than to salt. The model overcomes the problems of geometry and permeability outlined above by circumventing them and driving the system towards an isotonic solution by effectively combining the paracellular fluid flow and the pumped salt. The quasi-isotonic steady-state represents a very small hyperosmolarity across the cell which is required to provide the input to the osmosensor. (Osmotic equilibration similarly cannot generate a perfectly isotonic fluid). In this state the system is functioning as a zero osmotic clamp. Much of the behavior that is seen in epithelial fluid transport follows as a natural consequence. In the quasi-isotonic state the osmotic gradient across the cell is almost abolished and therefore transcellular osmosis is very small. This is why the probe studies yield the result that virtually all the volume flow occurs through the paracellular system.

In this paper we apply a protocol to the *in vitro* SMG system which does not seem to have been much used before on secreting epithelia. Hypertonic challenge in the basal perfusate has been used before [37] to calculate osmotic permeabilities from initial transients in the secretion rate. The results were interpreted in the context of osmotic fluid production. This is the measurement of fluid rates after a change in osmolarity of the source bath, created by an impermeant (or poorly permeating) solute, here sucrose. It should be noted that the whole paracellular pathway does not have to be impermeable to sucrose, and probably is not, but sucrose does have to be inaccessible to the mechanism responsible for driving salt through the JFT by an active process. Former experiments with this system, in which the size of paracellular probes entering the JFT system was measured, indicate that sucrose should be excluded on steric grounds [18]. We do not enter here into the details of the tight junction structure which are only partially understood. For clarity in what follows, however, it is important to differentiate between three transport or permeability elements of the junction which can be thought of as acting in parallel and which follow from experimental data. (i) Passive paracellular channels responsible for allowing small non-electrolytes and ions to cross. They are responsible for the high electrical conductivity of ‘leaky’ epithelia [5] and shunt permeabilities of small molecules. (ii) A non-selective channel for large molecules which may well represent the dropout and turnover of epithelial cells [32]. (iii) The system which is responsible for the net transport of paracellular probes (as opposed to their passive uni-directional permeation) and which must transport water and presumably ions [10, 25]. It is this pathway which is referred to frequently in this paper as the JFT

system and which is the essential component of the osmosensor feedback model investigated here.

Associated with this pathway is a selectivity, designated by θ , whose range is from 0 to 1 and which has the following property: when water and ions enter it from a bath of concentration C_s they are effectively transported at a lower concentration $C_s\theta$. By analogy with ultrafiltration the transported fluid is hypotonic because the solute is selected against, relative to water. Solute radius plays an important part here and it is this system which excludes sucrose.

We now examine the basis of the experiments and the possible results. We define a relative tonicity O_s of the transported fluid as

$$O_s = j_s / (J_v C_s) \quad (1)$$

where j_s is the transepithelial cellular salt flow, J_v is the transepithelial volume flow (secretion) and C_s is the salt concentration of the basal source bath (perfusate). When the system is functioning strictly isotonicly $O_s = 1.00$. We assume that the system is transporting near-isotonicly, whether it is operating by osmotic equilibration or by the JFT system described above.

In the osmotic case the concentration of secreted fluid will initially be $O_{s1}C_s$. When the bath is made hypertonic with an impermeant solute at concentration C_i the secreted steady-state salt concentration, assuming that the salt pumping has not altered during the time of the protocol, will now be equal to $O_{s2}(C_s + C_i)$. The fluid rate will therefore change from $J_{v(1)}$ to $J_{v(2)}$ such that the fractional reduction H is given by

$$H = \frac{J_{v(2)}}{J_{v(1)}} = \frac{O_{s1}C_s}{O_{s2}(C_s + C_i)}. \quad (2)$$

On the other hand, if the JFT system is in operation, salt will be transported through the paracellular system as well as water in addition to salt pumping through the cell. The selectivity θ of the system will determine how much salt is transported along with water and this will initially be close to $J_v C_s \theta$. When the osmotic clamp is in operation the epithelial water flow will be virtually all paracellular, in which case the cellular salt flow j_{sc} will be the difference between the epithelial and the paracellular salt flows, i.e. $j_{sc} = J_{v(1)}O_{s1}C_s - J_{v(1)}C_s\theta$ before the impermeant is added and $j_{sc} = J_{v(2)}O_{s2}(C_s + C_i) - J_{v(2)}C_s\theta$ afterwards. These will be equal if the cellular pumping has not changed, from which it follows that

$$H = \frac{J_{v(2)}}{J_{v(1)}} = \frac{O_{s1}C_s - C_s\theta}{O_{s2}(C_s + C_i) - C_s\theta} \quad (3)$$

which is a comparable expression to Eq. 2 but now includes the selectivity θ . Obviously, if there is little change in fluid tonicity then $O_{s1} = O_{s2}$ and the equations simplify a little. Measurement of H will

then indicate how far the system differs from a purely osmotic system. It also allows a measurement of θ to be made and this may be compared with the value of this parameter, which has been estimated from previous experiments on the SMG gland using graded paracellular probes. It should be noted that the two systems described here are ideal cases of the relation between H and the applied hyper-osmolarity ($C_s + C_i$): both are quasi-isotonic; the osmotic model behavior of Eq. 2 is purely cellular and that of Eq. 3 is virtually paracellular. In the subsequent discussion it will prove interesting and necessary to examine the behavior of H in model simulations that are run by using actual values of the cell parameters.

Experiments where the source bath osmolarity has been changed have usually been restricted to the measurement of the secreted fluid osmolarity, and this still remains isotonic although it contains no sucrose, this solute being replaced by salt in the secretion [3]. It is generally accepted that the rate of fluid transfer must decrease when the source bath is made hypertonic but rates are very hard to measure in epithelia over short times because they cannot usually be measured with sufficient time resolution. The *in vitro* perfused SMG preparation offers the great advantage that it represents a very large area of epithelium (concentrated into a spherical mass) that transports only when turned on with a secretory agonist and with a high rate of fluid flow leaving a small duct that can be connected to a measuring system. The time resolution is quite sufficient to follow fast changes in flow rate.

In addition to these experiments with normal rat glands we have had access to specially bred strains of rat in which AQP5, the principal aquaporin of the acinar cells, is either expressed in very low amounts in the gland or is present at intermediate levels. Differences between SMG preparations from normal and reduced AQP5 rats in response to hypertonic challenge can be measured and the resulting value of H compared with the predictions of both osmotic and feedback theories. An interesting feature of the low AQP5 rat strain is that this aquaporin can be shown to be deficient on the basal membrane of the cell, not the apical. The reasons for this are obscure but may relate to delivery of AQP5 to the basal membrane [19].

Another set of experiments was also performed to test the effects of Hg^{2+} ions, a potent inhibitor of AQP5, on the apical membrane. SMG preparations *in vitro* were subjected to retrograde injection of Hg^{2+} at different concentrations through the cannulated duct system. The effects of this on the flow rate before and after hypertonic challenge were measured, which permit a determination of H to be made. The results of this study therefore differ from those performed with knockout mice [15] in which the AQP5 is

completely absent and they permit differentiation between the effects of modulating basal and apical AQP5 on the fluid transport system.

Materials, Methods and Modelling

MATERIALS

Phenylmethyl sulfonyl fluoride (PMSF) and aprotinin were procured from Wako Pure Chemicals Ind. Ltd. (Osaka, Japan). The Bio-Rad protein assay kit was obtained from Bio-Rad laboratories (Hercules, CA). CompleteTM EDTA-free protease inhibitor cocktail tablets were purchased from Boehringer Mannheim GmbH (Mannheim, Germany). Fuji RX X-ray film was purchased from Fuji Film Co (Kanagawa, Japan). APS-coated micro slide glasses and micro cover glasses were purchased from Matsunami Glass Ind. Ltd. (Osaka, Japan). The donkey anti-rabbit IgG, horseradish peroxidase conjugated, was purchased from Amersham Pharmacia Biotech UK Ltd. (Buckinghamshire, England). Anti-rat AQP 5 antiserum was prepared in our laboratory [21, 29]. Salts, glucose, and HEPES were obtained from Nacalai Tesque Inc. (Kyoto). Carbamylcholine chloride (Carbachol, CCh) from Sigma (MO). A fluorine-fiber tube (EXLONTM) was purchased from Iwase Co. Ltd. (Atsugi, Japan).

ANIMALS AND AQP-5 DETERMINATION

Adult male Sprague-Dawley rats, weighing 250–350 g, (Shizuoka Laboratory Animal Center) were fed a standard pellet diet and water *ad libitum*. They were anesthetized by ether inhalation and the submandibular glands were removed from each rat. The levels of AQP-5 in the removed glandular tissue were determined by Western Blotting. The intact companion glands were used for fluid secretion studies.

The total membrane fraction of dissected tissue was prepared as previously described [20]. The tissues were homogenized in 9 vol. (w/v) of ice-cold homogenization buffer (5 mM HEPES buffer [pH 7.5], 50 mM mannitol, 10 mM MgCl₂, 1 mM PMSF, 1 µg/ml aprotinin, 2 µg/ml pepstatin A, 2 µg/ml leupeptin, and 1 tablet of CompleteTM EDTA-free protease inhibitor cocktail per 25 ml of buffer). The homogenate was filtered through a nylon mesh (150 mesh) and centrifuged at 800 × g for 10 min at 2°C to remove the nucleus and debris. By centrifugation of the supernatant at 200,000 × g for 1 h at 4°C, the pellet was collected as total membrane fraction and re-suspended in the homogenization buffer.

Protein in the total membrane fraction was determined by a Bio-Rad protein assay kit using bovine serum albumin as a standard. Antibodies used in the present study were prepared in our laboratory as described previously [21, 29]; they were raised by injecting rabbit with a mixture of Freund's complete adjuvant containing *M. butyricum* and C-terminal peptides of AQPs conjugated with keyhole limpet hemocyanin.

Protein samples of 5 µg and standard molecular weight protein markers were electrophoretically resolved in 12% polyacrylamide slab gels. After electrophoresis, the proteins separated on the gel were transferred onto a nitrocellulose filter by means of a Bio-Rad Mini Trans Blot apparatus (Hercules, CA) [30]. The blotted filter was blocked with 1% skim milk, probed with anti-AQP5 antiserum diluted 1,000-fold. In each experiment, a single lane was separated from the major part of the filter and incubated with the same concentration of antiserum that had been treated with 40 µg/ml of peptide (control experiment to verify the specificity of positive bands). Filters were next incubated with 3,000-fold diluted anti-rabbit IgG labelled with peroxidase, then with chemical

luminescence (ECL Detection Kit), and finally exposed to X-ray films. The visualized AQP band was scanned into a computer, and expression levels of AQP were determined by densitometric analysis using NIH Imaging software.

First-generation rats were separated into two groups, one is expressing a high level of AQP5 and the other, a low level of AQP5. The second generation (F1) was produced by mating within the latter group. Brother-sister mating between F1 animals was then conducted to obtain third-generation animals. In the present study we used a group of third to sixth generation rats with very low AQP5 expression.

PREPARATION OF SALIVARY GLANDS

The rats were anesthetized with pentobarbitone sodium (50 mg/kg body weight, by intraperitoneal injection). The submandibular glands (140–250 mg) were surgically isolated as previously described [17] and the attached sublingual gland was removed after ligation of the branches of feeding artery and draining vein. The extralobular main duct from the submandibular gland was cannulated with 0.3 mm I.D. × 0.5 mm O.D. (EXLONTM) for sampling. The artery distal to the glandular branch was cannulated with a stainless steel catheter (26G) connected to the infusion line for perfusion. The vein from the gland was cut freely. The gland was isolated and transferred to an organ bath (37°C), where the arterial catheter was connected to the perfusion apparatus. The drained venous effluent was continually removed.

The glands were perfused arterially at a rate of 2 ml/min using a peristaltic pump (Cole-Palmer) to supply enough oxygen even without specific oxygen carrier during the secretory phase [17]. The perfusion fluid was a buffered salt solution of the following composition (mM): Na⁺, 145; K⁺, 4.3; Ca²⁺, 1.0; Mg²⁺, 1.0; Cl⁻, 123.3; HCO₃⁻, 25.0; glucose, 5.0. This solution was buffered at pH 7.4 with 10 mM HEPES. For each experiment, this solution was made up from stock solutions and placed in a reservoir where it was equilibrated with a gas mixture of 95% O₂:5% CO₂.

In experiments with Hg, HgCl₂ was dissolved in the perfusate at 1, 10, 100 µM. 50 µl of solution was retrogradely injected into the excretory duct by a short cannula and left for 10 min. Thereafter the cannula was changed to a long cannula for measurements of fluid secretion.

FLUID SECRETION MEASUREMENTS

To observe fluid secretion, the ductal cannula was filled with perfusate buffer and the tip placed under the surface of water in a cup on an electronic balance (Shimadzu AEG-220), avoiding any contact with the bottom of the cup. Then, when the salivary secretion started, the cumulative secreted mass could be measured. Cumulative weight was automatically measured every 3 s and transferred to a computer. The rate of fluid secretion was calculated from time-differentiation of the cumulative volume of saliva assuming a saliva specific gravity of 1.0.

After control perfusion for longer than 20 min, recording started 5 min prior to the start of stimulation. Fluid secretion was induced by addition of 1 µM carbamylcholine (CCh) in the perfusate. After control stimulation with CCh for 10 mins, sucrose was added to the perfusate at the final concentration required for the hyperosmotic challenge which was continued for 10 min during continual CCh stimulation.

MODELLING

The equations of the feedback model are put into an Appendix together with estimates of the dimensions of the rat SMG acinar

cell and the osmotic permeabilities of the membranes, the cell pumping rate and the junctional selectivity. The equations were written in *Mathematica* (Wolfram Research) in two forms: (i) a steady-state model in which the simultaneous equations were solved under different conditions, and (ii) a 'perturbation' model in which a steady state was first established and then the effect of a step change in conditions was followed during a succession of time intervals, eventually leading to a new steady-state. This second form was used to emulate the actual time course of the changes seen in an experiment and this not only provided an explanation of acinar changes which might otherwise be difficult to understand but also showed that the parameter choices were essentially correct.

The osmotic model was run by turning off the feedback loop within the system and leaving all the passive parameters in place, enabling the system to work purely osmotically within the permeabilities of the cell and with the same pumping rate of salt. Thus the paracellular model is in essence an osmotic model with an osmosensor and linked JFT system added.

Results

Figure 1 shows the results of AQP5 localization in the SMG acini of the two strains used in this paper representing high (or normal) and low expressers of AQP5. Figure 1A shows AQP5 strongly expressed all over the acinar membrane, on both apical and basal membranes. Figure 1B shows that in the low expresser strain the AQP5 is still expressed at the apical membrane but very weakly, if at all, on the basal membrane.

Figure 2 is the record of an experiment in which a perfused *in vitro* gland has been stimulated to secrete with 1 μ M carbachol and at 10 min subjected to a hypertonic saline change from 0.3 M salt to 0.3 M salt + 0.03 M sucrose. The flow rate falls steeply but recovers to a new steady state. It is an interesting feature of this protocol that the new hypertonic state is usually more stable. The true fall has been estimated by back extrapolation to the point of intersection to compensate for changes in slope. At 20 min the hypertonic saline is replaced with the former saline when there is a sharp rise to the former state with an overshoot and at 25 min the carbachol is removed.

Figure 3 is a perturbation generated by the feedback model for the hypertonic challenge. It can be seen that the undershoot and rise to a new steady state (A) is reproduced in the simulation. This requires an addition to the basic model (as might be applied to the epithelium alone) to incorporate volume changes in the sub-epithelial and ductal baths, as discussed below. If this additional feature is not incorporated then there is no undershoot and the transition to the new steady state is monotonic but the new flow rate has the same value. Thus the transition can be understood as not being a cellular or epithelial feature *per se*.

In Figure 4 a hypertonic challenge experiment can be seen with sucrose at three concentrations

(0.02, 0.04 and 0.06 M) added to a saline of osmolarity 0.3. The fraction flow H is seen fitted to Eq. 3 for a θ value of 0.77. On the same graph is plotted Eq. 2 which actually represents the minimum values for H as a function of the basal osmolarity C_b equal to $(C_s + C_i)$. Any departure from isotonicity during osmotic equilibration towards a more hypertonic secretion will lead to a line with higher H values, so the line here can be regarded as the absolute limit for the osmotic model. It must be clear that the results show that the data fit the paracellular model remarkably well and not the osmotic model. The value of the selectivity θ , as well as being the fitting parameter within the paracellular model of Eq. 3, is also very close to the value that can be obtained independently from experiments with graded paracellular probes [18] as discussed below.

Figure 5 is a similar plot of the results obtained for rat SMG with very low AQP5 status, compared with a different set of normal SMG as controls. It can be seen that the normal AQP5 preparations again show a similar value completely outside the osmotic range, but the low AQP5 preparations are now osmotic conformers. The osmotic curve is not that of the minimum or 'osmotic envelope' of Fig. 4 but is generated by the osmotic model in which estimated values of the membrane P_{os} are used. This is because the preparation is now deficient in AQP5 at a critical membrane and can no longer be assumed to produce an isotonic secretion as required by the criterion of Eq. 2. Apart from supporting an osmosensor-JFT model these results give strong support that the osmosensor, in this tissue at least, is an aquaporin situated at the basal membrane, for this is the membrane which histological analysis has shown is deficient in the low AQP5 strain used here [19].

Figure 6 shows the results of similar hypertonic challenge experiments with a group of rat SMG preparations in which the AQP5 levels were assayed as intermediate. The sucrose levels were here as high as 0.06 M and the H values of these fall within the expected range of those SMG preparations with normal AQP5 levels. In this case there does not seem to be a graded response to lowered AQP5 levels.

Figure 7 represents the effects of retrograde injection of Hg^{2+} solutions of increasing strength into the cannulated duct of the gland before induction of fluid flow. In these experiments there is almost certainly a back-pressure created (initially) but the glands still transport and show responses to hypertonic challenge in the expected range for normal AQP5 preparations. In Fig. 7a the secretion rate prior to challenge (i.e., the carbachol-induced flow rate at 10 min) can be seen to decline in a manner graded with the Hg^{2+} concentrations consistent with inhibition of an aquaporin that is contributing to the osmotic permeability of the apical membrane. Fig. 7b shows H values, which are all similar to the controls,

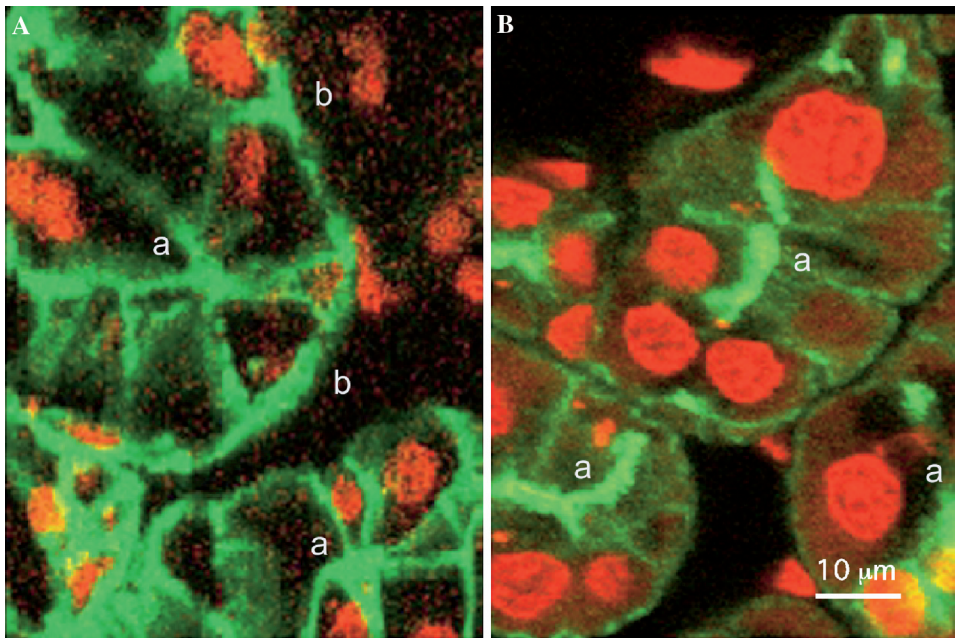


Fig. 1. Fluorescent antibody localization of AQP5 in two sections of SMG acini from strains with different expression levels. (A) High-expression rats in which strong staining is apparent of both apical (*a*) and basal (*b*) membranes of the acinar cells. (B). Low-expression rats in which significant expression is apparent only at the apical (*a*) membrane. Calibration bar: 10 μm .

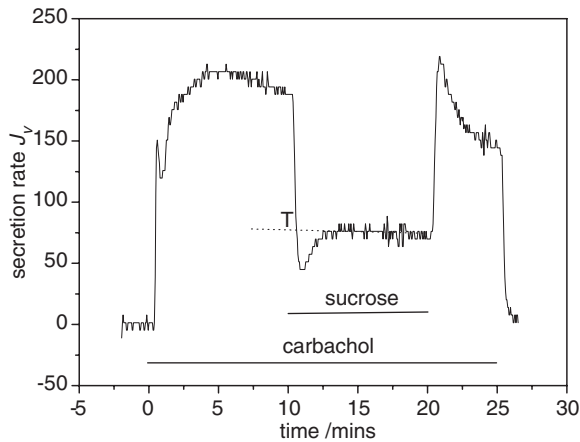


Fig. 2. A typical experiment showing the onset of fluid secretion after carbachol with the perturbation caused by hypertonic saline perfusion (60 mOs sucrose). The new steady-state value was estimated by back extrapolation to the point *T* at 10 min. The effect of sucrose is reversible, taking into account the decay of secretion rate with time.

showing no significant change with increasing Hg^{2+} concentration. These *H*-values are far too low to be explained in terms of osmotic equilibration. The effects of apical Hg^{2+} application indicate that although the osmotic permeability due to AQP5 influences the fluid secretion rate, the osmosensor-JFT system is still in operation. We shall argue below that this result can be understood in terms of the model, which can reproduce this behavior, but it is not compatible with simple osmotic equilibration.

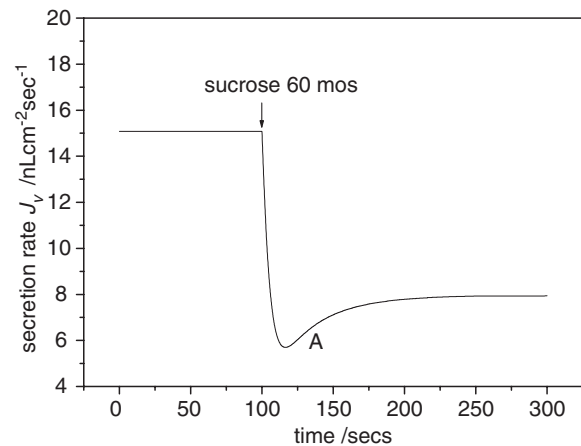


Fig. 3. A transient induced by 60 mOs sucrose addition to the perfusate, generated by the time-dependent version of the sensor-JFT model with basic parameter values.

Discussion

The initial result of imposing a hypertonic challenge at the basal membrane of the acinar cell, as can be seen in Fig. 2, is to cause an initial fall in flow rate with an undershoot followed by a rise to a new steady state. This undershoot is not due to changes in transport of salt and water in the epithelium per se, for using the osmosensor-JFT model without additional assumptions does not reproduce this effect but indicates a smooth fall to a new steady state. It is important to know whether this indicates that the model is lacking

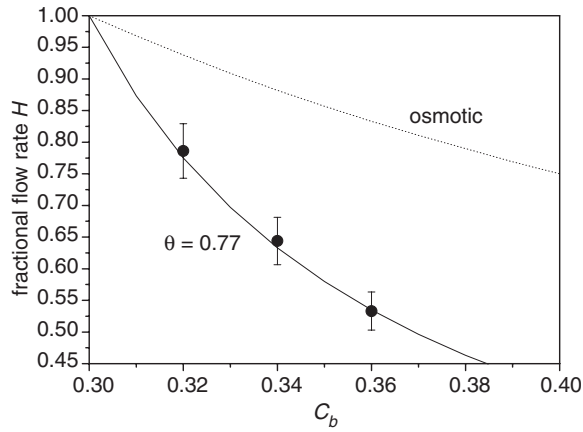


Fig. 4. Normal SG rat preparations. Plot of the rate ratio H for saline with 20, 40 and 60 mOs sucrose additions. The fitted curve is that of Eq. 3 with a selectivity of 0.77. The osmotic line is the minimum value of H calculated from Eq. 2 for an isotonic fluid, i.e., when $Os_1 = Os_2 = 1$.

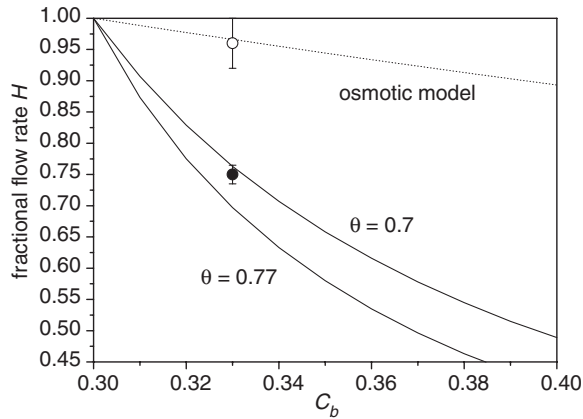


Fig. 5. Low AQP5 rat preparations (○) and normal controls (●). Plot of the rate ratio H for saline with 30 mOs sucrose addition. The lower curves are generated by the model with basic parameters and the selectivities shown. The upper osmotic curve (dotted) is generated by the model with similar basic parameters but the gain A set to zero.

some feature. It appears that this effect is due to cell swelling within the acinus and when a simple scheme for this is added to the basic epithelial model the undershoot can be reproduced. The important feature is that, with or without this addition, the new steady state is the same. When a hypertonic challenge is applied by perfusion the acinar cell immediately begins to shrink and this volume decrease will be partially transmitted inwards to the acinar lumen, causing it to widen. If the epithelium is secreting into the lumen at a rate j_1 and the initial rate of increase in luminal volume due to shrinkage is j_{lum} then the apparent rate of secretion will fall to $(j_1 - j_{lum})$. As the cell equilibrates to a new volume, j_{lum} will decay away to zero to reveal

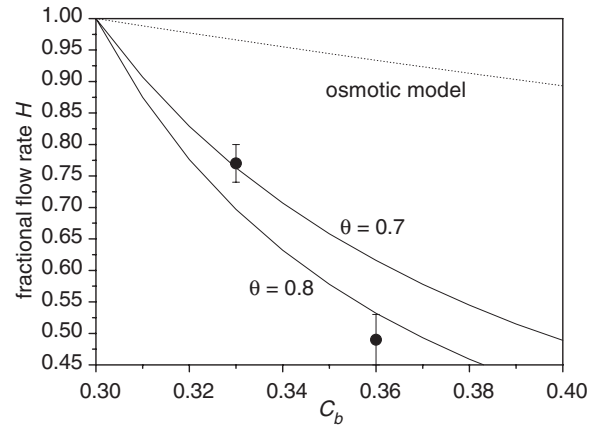


Fig. 6. Intermediate AQP5 rat preparations. Plot of the rate ratio H for saline with 30 or 60 mOs sucrose addition. The lower curves are generated by the model with basic parameters and the selectivities shown. The upper osmotic curve (dotted) is generated by the model with similar basic parameters but the gain A set to zero.

the epithelial secretion rate which is now changing to a new steady-state value j_2 . Incorporating the cell changes into the perturbation version of the model is relatively simple and has been done by calculating the change in cell volume at every step of the evolution and partitioning this symmetrically between basal and apical sides of the cell. This procedure is straightforward and reproduces the swings of secretion rate between the steady states very well. The details are found in the Appendix.

NORMAL GLANDS

The results for normal glands (Fig. 4) indicate that the data is a consistent fit to the JFT model and cannot be explained by osmotic equilibration. We have commented above that the fitted curve for the JFT model uses a value for θ of 0.77 as a fitting parameter and this value has been obtained from a former study on rat SMG in experiments which are quite different to the protocols used here. This study is one in which the paracellular pathway was probed with a series of dextrans of different radii and should be consulted for the details of the procedure [18]. Briefly, the paracellular probes that cross the junction exhibit a net flux or secretion which falls off with increasing molecular radius, as determined by size partition chromatography. The net flux, which must be via the convective JFT system, is linear and indicates a cut-off radius beyond which small molecules cannot pass the junctions by this route. Similar cut-off radii have been determined for other fluid-transporting epithelia [26] and lie between 5–6 Å. This behavior is described by a steric exclusion factor [10, 22] which for a solute of radius r_s in a parallel channel of half-separation r_{ch} is

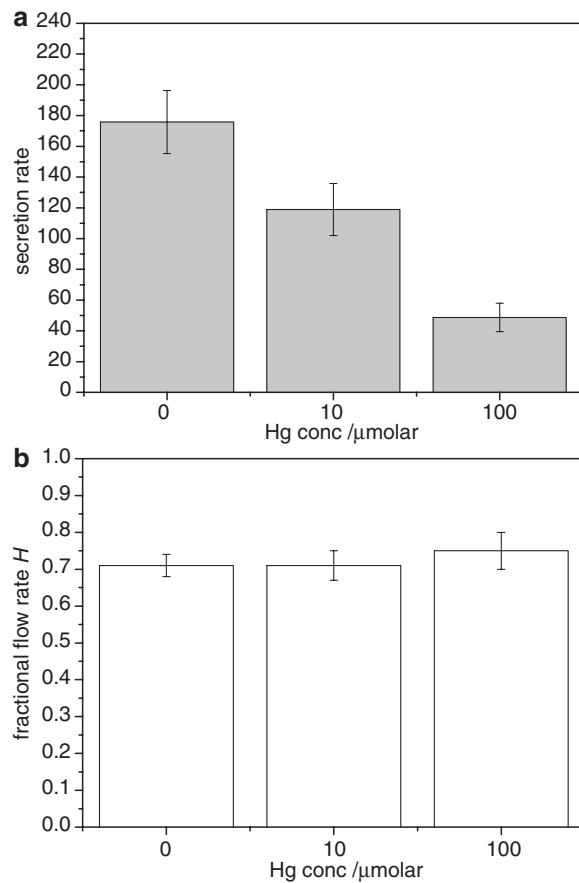


Fig. 7. (A). The secretion rate of normal rat preparations after retrograde ductal injection with Hg. The rates after 10 min carbachol stimulation show a progressive decline with Hg concentration. (B). The rate ratio H measured after 30 mOs sucrose challenge. There is no significant rise value with rising Hg concentration.

$$S = (1 - r_s/r_{ch}) \quad (4)$$

and the selectivity will be the ratio of the S factors for salt and water, i.e.,

$$\theta = S_s/S_w. \quad (5)$$

Using a channel width of 5.5 \AA [18], a water radius of 1.5 \AA and a mean hydrated radius between Na^+ and Cl^- of 2.3 \AA we obtain a value of 0.8 for θ . Slightly different values can be obtained with a somewhat different ionic radius but the values for θ are comparable. This value is virtually the same as that obtained in the hypertonic challenge experiments reported here and gives strong support to the paracellular model. In essence it confirms that the JFT properties, which were derived independently from permeation studies, are similar to those required by paracellular fluid production. The osmotic theory has no explanation for this correlation.

The value of 0.77 for θ has other implications. It indicates that the fraction of salt passing the paracellular system with the water is 77% of the total secretory salt. It may come as a surprise to realize this implication of the model but it is a natural consequence of the JFT system and this level of selectivity. Where the pump fraction of the transepithelial net Na flux has been measured in an isotonic leaky fluid-transporting epithelium (*Necturus* gallbladder) by flux analysis, it reveals that only 35% of the salt secretion is cellular [8, 9] and a similar fraction (31%) is obtained by measuring the rise of Na in the cell after ouabain inhibition of the pump with ion-sensitive Na microelectrodes [9]. In other studies with the same epithelium the ion-sensitive microelectrode technique yielded similar values of 42% [14], 31–36% [36] and 41% [23]. These studies have been analyzed and discussed in some detail [9].

LOW-AQP5 GLANDS

In Fig. 5 the behavior of SMG preparations in hypertonic challenge experiments using rats selected for very low AQP5 expression are compared to rats from the same stocks whose levels were normal. The differences were striking: compared to glands with normal expression levels the low AQP5 glands show H values to be expected from the osmotic equilibration model. In these experiments with glands in vitro the low AQP5 preparations showed secretion rates which were reduced to 46% of the normal. The figures from these experiments are similar in overall secretory reduction to salivary glands with AQP5 knockout [15], which fell to about 41% and produced a secretion with a mean hypertonicity of about 1.43. Clearly AQP5 deficiency at the basal membrane is affecting the mechanism of fluid secretion and from the hypertonic data it appears to be switching this from a JFT feedback system to an osmotic one which operates at a lower rate.

This situation can be generated quite straightforwardly from the basic model. By removing the feedback loop between the osmosensor and the JFT, as would happen if the sensor function of AQP5 were removed, the curves for H alter from those that fit the normal AQP5 preparations to the line designated as ‘osmotic model’ in Fig. 5. In addition, the osmolarity rises from $O_s = 1.003$ to 1.38 indicating that, using the parameters of the basic model incorporating P_{os} values for the two membranes of 10^{-2} cm/s (close to that of the human red cell), the osmotic model creates a hypertonic secretion without feedback, i.e., by pure osmosis.

AQP5 assays from the stocks used in these experiments were compared by Western blotting densitometry and the lowest values, from inbred low stocks, were 7% of those from high [19]. Immunohistochemical localization of AQP5 is shown in Fig. 1

and indicates that the low AQP5 acini are deficient in AQP5 at the basal membranes compared to the normal ones. Although in some work AQP5 has not been localized in the basal membrane of rat SMG (discussed in [19]), here it clearly was. The reduction of basal AQP5 may be created by a failure of sorting to the basal membrane as it appears in the apical membrane. Whatever the cause, the apparent loss of osmosensor control of fluid transport and AQP5 basal deficiency in this strain indicates that the osmosensor is AQP5, signalling from that membrane rather than the apical membrane. This is in conformity with the assumptions of the model.

Amongst rats chosen for these experiments were some which may be termed ‘intermediate’ in the AQP5 assay, some having AQP5 levels of 27% of the levels from normal rats. The mean assay of this group was 64% of the highest members. In Fig. 6 the results of hypertonic challenge experiments on this group can be seen in which some were subjected to a hyperosmotic step of 60 mOs. The results indicate that there is no approach to an osmotic model. This indicates that a partial reduction of AQP5 levels does not lead to a loss of feedback. However, if the mechanism of fluid production were osmotic a partial reduction in flow rate would be expected. The pre-challenge secretion rates in this group were 142 ± 15 compared to 140 ± 10 for all normal rates. We suggest that it is only when osmosensor levels become very low that feedback control is lost and that the variation seen in AQP5 assays in this group is not enough to come near this position.

Once again this can be followed with the behavior of the osmosensor model. In the basic parameters the gain is set to $A = 10$ with the sensor density m equal to 1 (see Appendix). When the overall gain product Am is reduced towards zero it is only between 2 and 0 that any effect is seen on either the fluid transport rate J_v , the osmolarity ratio Os , or the value of H . The value of Am is a controlling parameter value which represents the strength of the control loop. The crucial point is that the effect of Am is highly non-linear and soon begins to saturate in an asymptotic manner. It is very probable that cells have a level of sensor that is higher than needed to ensure isotonic functioning of the epithelium and that the feedback loop works quite well with different expression levels until m becomes very low indeed.

RETRO-PERFUSION WITH HgCl_2

In experiments where HgCl_2 was added to the saline and injected up the duct the aim of the protocol was to inhibit the AQP5 at the apical membrane prior to hypertonic challenge perfusions. If the AQP5 at the apical membrane was acting as part of the feedback loop, it should have an effect on H . With retrograde injection there is the problem of knowing the exact

Hg^{2+} concentration at the apical membrane as the perfusate and the secreted fluid commingle. The results are collected in Fig. 7 and show two effects. (i) In Fig. 7a the secretion rate J_v falls with increasing Hg^{2+} concentration, and (ii) In Fig. 7b the hypertonic challenge leads to an H value which is similar in magnitude to normal SMG preparations and which does not significantly change with Hg^{2+} concentration.

There is a progressive fall in J_v with rising Hg^{2+} concentration at the apical membrane, which can be explained by the fact that only a fraction of the actual Hg^{2+} concentration in the perfusing pipette is present at the apical membrane due to dilution, and this fraction is not quantifiable. The absolute values of the fall in J_v indicate that the progressive inhibition of AQP5 is having an effect. However, the H value is similar to normal preparations and shows no significant change with rising Hg^{2+} . By itself, this lack of change in Fig. 7b would indicate that the inhibitor is not reaching the AQP5 sites, but this cannot be the case, as Fig. 7a demonstrates. The absolute value of H shows that the mechanism is not compatible with the osmotic model and indicates that the JFT system is still in operation. The question then resolves as to whether the osmosensor-JFT model can explain both effects.

In these conditions the model displays the following behavior. If the osmosensor is situated on the basal membrane of the acinar cell then during steady-state operation of the feedback system the input signal is due to the difference in osmolarity between the basal perfusate and the cell. When the apical membrane permeability P_a is lowered by inhibition (with Hg^{2+}) the input signal decreases because the cell osmolarity C_c is becoming progressively cut off from contact with the apical bath osmolarity C_a (the secretion) and dominated by that of the basal bath C_b (Appendix, Eq. A2). The cell osmolarity approaches C_b , decreasing the input signal ($C_c - C_b$), and the osmosensor turns down the JFT system and therefore the secretion rate declines. Thus, in terms of an osmotic equilibration, the system behaves as though osmotic flow were being decreased but in terms of the osmosensor model, it is the paracellular flow that is decreasing due to a lowering of the feedback signal. The model indicates that secretion rates prior to hypertonic challenge will be smaller with rising inhibitor concentration (Fig. 7a) but the H values in response to hypertonic challenge will be virtually unchanged because the feedback system is still operating, and with a selectivity θ close to 0.8. The experimental results confirm this.

These results indicate that the AQP5 at the apical membrane is not acting as an osmosensor because if this were so the H values would rise towards those of an osmotic system as shown in Fig. 5. The flow rates show a dependency upon the osmotic permeability of

the apical membrane due to its contribution to the regulation of cell osmolarity [12].

CONCLUSIONS

To summarize, the experiments have shown the following.

- (i) Hypertonic challenges to the perfused basal membrane of SMG acinar cells elicit a fractional decrease in fluid secretion rate H that is incompatible with an osmotic model of fluid transport but which is uniquely explained by a proposed osmosensor feedback model in which most of the volume flow is paracellular.
- (ii) The selectivity θ of the JFT system used to fit the responses is very similar to that derived from previous experiments using paracellular molecular probes of differing radius. This agreement strongly suggests that the paracellular system is the dominant route for water transport during secretion.
- (iii) SMG glands from rats of low AQP5 expression at the basal membrane show H values on hypertonic challenge close to those expected for a scheme of fluid secretion by cellular osmosis. This indicates that basal AQP5 is probably the osmosensor controlling a JFT system and that feedback is lost when the normal expression of this molecule is considerably impaired.
- (iv) Inhibition of apical AQP5 with Hg^{2+} ions has an effect on fluid secretion rates and H -values that is not compatible with simple osmotic flow but which is consistent with an osmosensor system located at the basal membrane.

Appendix

THE OSMOSENSOR-JFT MODEL AND THE SALIVARY EPITHELIUM

The model presented here is one that has been suggested previously [26] and is developed for a forward-facing epithelium in this issue [12] in which the behavior has been explored. Here we apply the principles with a minimum of adaptation to the SMG gland, a backwards-facing epithelium that transports from serosa to lumen (Fig. A1). Two forms of the model have been developed, a steady-state solution and a time-dependent system used to investigate the changes that occur when a perfused gland in a steady state is subjected to a step change. Central to the model is the JFT (junctional fluid transfer) system which is considered to be the basis

of fluid production in isotonicity transporting epithelia [26]. This fluid transfer pathway is located in the junction but is functionally different from the leak pathway with which it may be considered to be in parallel. The JFT system implies the coupled transfer of water and solute, in particular the NaCl of the bathing saline. The pathway has a selectivity θ which represents the ratio of salt:water transferred compared to the ratio in the source bath. The JFT rate is controlled by a membrane osmosensor, ideally located at the membrane separating source bath and cell, here considered to be AQP5 at the basal membrane.

STEADY STATE

The feedback model is described by three linear simultaneous equations

$$jv_p = Am(C_c - C_b) + jvo \quad (\text{A1})$$

$$C_c = (P_a A_a C_a + P_b A_b C_b) / (P_a A_a + P_b A_b) \quad (\text{A2})$$

$$C_c = (jv_p C_b \theta + P_s (C_b - C_a) + j s_c) / (jv_p + P_a A_a (C_a - C_c)) = J_s / J_v. \quad (\text{A3})$$

The basic parameters in these equations are:

- jv_p junctional volume flow cm s^{-1}
- jvo junctional volume flow offset cm s^{-1}
- $j s_c$ trans-cellular pumping rate $\text{osmole cm}^{-2} \text{s}^{-1}$
- A gain of the feedback loop $\text{cm}^4 \text{osmole}^{-1} \text{s}^{-1}$
- m sensor density in the membrane
- $C_{a,b,c}$ apical, basal or cell osmolarity osmole cm^{-3}
- $P_{a,b}$ apical, basal osmotic permeabilities $\text{cm}^4 \text{osmole}^{-1} \text{sec}^{-1}$
- $A_{a,b}$ apical, basal membrane areas $\text{cm}^2 (\text{cm}^2 \text{epithelium})^{-1}$
- P_s solute permeability of the leak pathway cm s^{-1}
- θ selectivity of the JFT pathway

Eq. A1 describes the transduction of the osmotic signal input by a sensor and signaling sequence at the basal membrane into a junctional volume flow jv_p in addition to the offset, i.e., the rate at which the JFT transfers volume in the absence of the signal. In this paper jvo is set to zero. The sensor output depends upon its density m in the membrane and has a gain A .

Eq. A2 describes the osmotic concentration in the cell, which is the result of osmotic flow over the two membranes being equal in the steady state to preserve cell volume.

Eq. A3 describes the emergent fluid osmolarity, given as the ratio of transepithelial salt flow J_s to the overall fluid transport rate J_v . J_s is made up of three

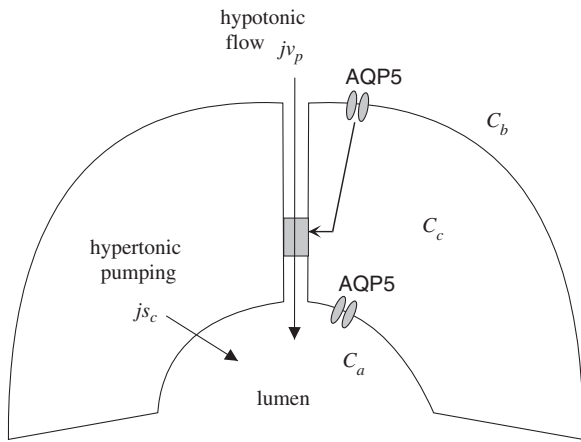


Fig. A1. Major features of the sensor-feedback model applied to SMG. Feedback control of the JFT system is proposed for the basal AQP5 acting as an osmosensor.

components. (i) $jv_p C_b \theta$ the convection of salt through the JFT driven by the fluid transport mechanism with a selectivity θ . (ii) $P_s(C_b - C_a)$ the salt diffusion between baths across the paracellular system where P_s is the overall permeability. In this paper P_s is set to zero because the leak pathway, although permeable to individual ions, has a low overall permeability to salt. (iii) js_c the rate of active salt pumping through the trans-cellular route. J_v is made up of two components. (i) the paracellular volume flow jv_p and (ii) the osmotic flow from cell to luminal space, $P_a A_a (C_a - C_c)$.

The parameters were given a standard set of initial values approximating to a general epithelial cell. In many transporting epithelia the apical membrane is much smaller than the basolateral membrane and this certainly applies to the acinar cells of most exocrine glands. Although the acinar epithelium is topologically spherical or tubular, the model has no geometry but the cell and interspace are given area and volume. This is not an important criterion because the dominant feature of the cell turns out to be the overall osmotic conductance of each membrane $P_a A_a$ and $P_b A_b$ and especially their ratio. The values for A_a and A_b used here are 1 and 10. The osmotic permeability is 2×10^{-2} for both membranes, close to the value for red cells. Salt is pumped across the cell by the general mechanism for backward-facing epithelia in which Na recirculation at the basal membrane drives the extrusion of Cl through the apical membrane [16]. The rate js_c for this was 2×10^{-9} mole s^{-1} per cm^{-2} epithelium, a moderate value for secretory epithelia. In this feedback model the general behavior is not affected by the magnitude of js_c and under isotonic conditions the pumping merely determines the overall fluid transport rate.

One of the most important parameters is θ the selectivity. Changes in this affect the proportion of salt

passing the JFT but not the tonicity of the fluid. The selectivity is also equal to the fraction of salt crossing the epithelium by the paracellular route under normal conditions. The paracellular salt flow is $jv_p C_b \theta$ and the transepithelial salt flow is equal to $J_v C_b$, so this fraction is given by $jv_p C_b \theta / J_v C_b$. As the system is functioning close to isotonicity then virtually all the volume flow is paracellular so that $jv_p = J_v$ and the paracellular salt fraction becomes equal to θ .

Finally, the gain A is the overriding parameter (strictly Am , as $m = 1$ here). We have no precise knowledge of this until we understand the coupling between the sensor and the JFT. However, when A is increased above zero we very quickly enter a state of ‘osmotic clamp’ where the relative osmolarity O_s becomes close to 1.0 and the transported fluid may be regarded as isotonic. In this condition the osmotic permeabilities of the membrane play little part and most of the fluid flow is paracellular. This isotonic condition is very stable and is independent of changes in the permeabilities, the geometry and the salt pumping rate of the acinar cells.

TIME-DEPENDENT VERSION

This version has been used to follow changes after hypertonic challenge shown in Fig. 3 by incorporating time-dependent elements. Briefly, the rise of concentration change adjacent to the basal membrane after switching salines is treated as a sub-epithelial diffusive compartment with a single exponential time constant λ with a half-time of 20 s. The osmosensor system has also an exponential time constant k with a half-time of 10 s. This represents the reaction of the sensing molecule (probably AQP5) and the cell signalling chain to the JFT system. These are estimates that can be justified on simple physical grounds. Finally, there is a volume V_{lis} assigned to the lateral interspace system around the cell, $0.5 \mu m$ wide and of cell height $25 \mu m$. Water flows are calculated over basal membrane, interspace membrane and apical membrane. The concentration of salt in the lateral interspace varies during transients but is dominated by C_b in the steady state.

As the cells shrink during hypertonic challenges the volume change will be distributed between lumen and the sub-epithelial side of the cell. The luminal volume shift will decrease the apparent secretion rate but this effect will decline as the cell equilibrates. The interspace concentrations are calculated in discrete time steps which determine the rate of salt transport by the JFT system and the osmotic exchanges with the cell. The cell volume at every step of the evolution is calculated and partitioned symmetrically using a factor $\beta = 0.5$ between

basal and apical sides of the cell. This procedure is straightforward and reproduces the swings of secretion rate between the steady states quite well. When β is set to zero the undershoot of Fig. 3 is not seen.

The time step lengths were systematically explored and the curve of Fig. 3, which is similar in magnitude and time to the experimental data of Fig. 2, was generated by using the above values of β , λ and k . Damped oscillations on entry to the new steady state could be generated by adjusting the values of λ and k as might be expected for a feedback system. These oscillations can be seen in many experiments during osmotic challenge. Together with other transients, they are indications that a feedback system is in operation and remain to be explored further.

References

- Case, R.M., Cook, D.I., Hunter, M., Steward, M.C., Young, J.A. 1985. Trans-epithelial transport of nonelectrolytes in the rabbit mandibular salivary-gland. *J. Membrane Biol.* **84**:239–248
- Curran, P.F., MacIntosh, J.R. 1962. A model system for biological water transport. *Nature* **193**:347–348
- Diamond, J.M. 1965. The mechanism of isotonic water absorption and secretion. *Symp. Soc. Exp. Biol.* **19**:329–347
- Diamond, J.M., Bossert, W.H. 1967. Standing-gradient osmotic flow: A mechanism for coupling of water and solute transport in epithelia. *J. Gen. Physiol.* **50**:2061–2083
- Fromter, E., Diamond, J.M. 1972. Route of passive ion permeation in epithelia. *Nature [New Biol.]* **235**:9–13
- Hernandez, C.S., Gonzalez, E., Whitttembury, G. 1995. The paracellular channel for water secretion in the upper segment of the Malpighian tubule of *Rhodnius prolixus*. *J. Membrane Biol.* **148**:233–242
- Hill, A.E., Hill, B.S. 1978. Sucrose fluxes and junctional water flow across *Necturus* gall bladder epithelium. *Proc. R. Soc. Lond. B.* **200**:163–174
- Hill, A.E., Hill, B.S. 1987. Steady state analysis of ion fluxes in *Necturus* gall bladder epithelial cells. *J. Physiol.* **382**:15–34
- Hill, A.E., Hill, B.S. 1987. Transcellular Na fluxes and pump activity in *Necturus* gall bladder epithelial cells. *J. Physiol.* **382**:35–49
- Hill, A.E., Shachar-Hill, B. 1993. A mechanism for isotonic fluid flow through the tight junctions of *Necturus* gallbladder epithelium. *J. Membrane Biol.* **136**:253–262
- Hill, A.E., Shachar-Hill, B. 1997. Fluid recirculation in *Necturus* intestine and the effect of alanine. *J. Membrane Biol.* **158**:119–126
- Hill, A.E., Shachar-Hill, B. 2006. A new approach to epithelial isotonic fluid transport: an osmosensor feedback model. *J. Membrane Biol.* **210**:000–000
- Hill, A.E., Shachar-Hill, B., Shachar-Hill, Y. 2004. What are aquaporins for? *J. Membrane Biol.* **197**:1–32
- Jensen, P.K., Fisher, R.S., Spring, K.R. 1984. Feedback inhibition of NaCl entry in *Necturus* gallbladder epithelial cells. *J. Membrane Biol.* **82**:95–104
- Ma, T.H., Song, Y.L., Gillespie, A., Carlson, E.J., Epstein, C.J., Verkman, A.S. 1999. Defective secretion of saliva in transgenic mice lacking aquaporin-5 water channels. *J. Biol. Chem.* **274**:20071–20074
- Melvin, J.E., Yule, D., Shuttleworth, T., Begenisich, T. 2005. Regulation of fluid and electrolyte secretion in salivary gland acinar cells. *Annu. Rev. Physiol.* **67**:445–469
- Murakami, M., Miyamoto, S., Imai, Y. 1990. Oxygen-Consumption For K^+ Uptake During Poststimulatory Activation Of Na^+ , K^+ -AtPase In Perfused Rat Mandibular Gland. *J. Physiol.* **426**:127–143
- Murakami, M., Shachar-Hill, B., Hill, A.E., Steward, M. 2001. The paracellular component of water flow in the rat submandibular gland. *J. Physiol.* **537**:899–906
- Murdiastuti, K., Miki, O., Yao, C., Parvin, N., Kosugi-Tanaka, C., Akamatsu, T., Kanamori, N., Hosoi, K. 2002. Divergent expression and localization of aquaporin 5, an exocrine-type water channel, in the submandibular gland of Sprague-Dawley rats. *Pfluegers Arch.* **445**:405–412
- Murdiastuti, K., Miki, O., Yao, C.J., Parvin, M.N., Kosugi-Tanaka, C., Akamatsu, T., Kanamori, N., Hosoi, K. 2002. Divergent expression and localization of aquaporin 5, an exocrine-type water channel, in the submandibular gland of Sprague-Dawley rats. *Pfluegers Archiv-Eur. J. Physiol.* **445**:405–412
- Parvin, M.N., Tsumura, K., Akamatsu, T., Kanamori, N., Hosoi, K. 2002. Expression and localization of AQP5 in the stomach and duodenum of the rat. *Biochim. Biophys. Acta-Mol. Cell Res.* **1542**:116–124
- Renkin, E.M., Curry, F.E. 1979. Transport of water and solutes across capillary endothelium. In: *Membrane Transport in Biology*. Vol. IVa. pp. 1–46. Springer-Verlag, NY
- Reuss, L. 1984. Independence of apical membrane Na^+ and Cl entry in *Necturus* gallbladder epithelium. *J. Gen. Physiol.* **84**:423–445
- Schnermann, J., Chou, C.L., Ma, T.H., Traynor, T., Knepper, M.A., Verkman, A.S. 1998. Defective proximal tubular fluid reabsorption in transgenic aquaporin-1 null mice. *Proc. Nat. Acad. Sci. USA* **95**:9660–9664
- Shachar-Hill, B., Hill, A.E. 1993. Convective fluid-flow through the paracellular system of *Necturus* gallbladder epithelium as revealed by dextran probes. *J. Physiol.* **468**:463–486
- Shachar-Hill, B., Hill, A.E. 2002. Paracellular fluid transport by epithelia. *Int. Rev. Cytol.* **215**:319–350
- Song, Y.L., Verkman, A.S. 2001. Aquaporin-5 dependent fluid secretion in airway submucosal glands. *J. Biol. Chem.* **276**:41288–41292
- Steward, M.C. 1982. Paracellular non-electrolyte permeation during fluid transport across rabbit gallbladder epithelium. *J. Physiol.* **322**:419–439
- Tada, J., Sawa, T., Yamanaka, N., Shono, M., Akamatsu, T., Tsumura, K., Parvin, N., Kanamori, N., Hosoi, E. 1999. Involvement of vesicle-cytoskeleton interaction in AQP5 trafficking in AQP5-gene-transfected HSG cells. *Biochem. Biophys. Res. Commun.* **266**:443–447
- Towbin, H., Staehelin, T., Gordon, J. 1979. Electrophoretic transfer of proteins from polyacrylamide gels to nitrocellulose sheets - Procedure and some applications. *Proc. Nat. Acad. Sci. USA* **76**:4350–4354
- Vallon, V., Verkman, A.S., Schnermann, J. 2000. Luminal hypotonicity in proximal tubules of aquaporin-1-knockout mice. *Am. J. Physiol.* **278**:F1030–F1033
- Van Os, C.H., Wiedner, G., Wright, E.M. 1979. Volume flows across gallbladder epithelium induced by small hydrostatic and osmotic gradients. *J. Membrane Biol.* **49**:1–20
- Verkman, A.S. 2000. Physiological importance of aquaporins: lessons from knockout mice. *Curr. Opin. Nephrol. Hypertension* **9**:517–522
- Verkman, A.S. 2002. Physiological importance of aquaporin water channels. *Ann. Med.* **34**:192–200

35. Verkman, A.S., Yang, B.X., Song, Y.L., Manley, G.T., Ma, T.H. 2000. Role of water channels in fluid transport studied by phenotype analysis of aquaporin knockout mice. *Exp. Physiol.* **85**:233S–241S
36. Weinman, S.A., Reuss, L. 1984. Na^+ - H^+ exchange and Na^+ entry across the apical membrane of *Necturus* gallbladder. *J. Gen. Physiol.* **83**:57–74
37. Nakahari, T., Steward, M.C., Yoshida, H., Imai, Y. 1997. Osmotic flow transients during acetylcholine stimulation in the perfused rat submandibular gland. *Exp. Physiol.* **82**:55–70